MULTIVARIABLE *LQG* VIBRATION CONTROL USING CHARGE-DRIVEN PIEZOELECTRIC ACTUATORS

Benjamin J. G. Vautier * **S. O. Reza Moheimani** *

* *School of Electrical Engineering and Computer Science, The University of Newcastle, NSW, Australia.*

Abstract: Piezoelectric actuators are known to exhibit hysteresis when driven at relatively large voltages. In most situations this phenomenon is detrimental. Electric charge is known to naturally reduce the effects of hysteresis. The interaction of charge driven piezoceramics with flexible structures is analyzed and reveals that the dynamics of the system are different from the voltage driven case. A procedure for obtaining a charge driven plant model is documented, which can be used with standard control design tools. A multivariable *LQG* charge controller is designed to reject disturbance vibrations acting on a cantilever beam. Experimental results demonstrating the effectiveness of this method are included.

Keywords: Actuators, Charge amplifiers, Structures, Vibration, Active control, LQG

1. INTRODUCTION

Piezoelectric transducers have become increasingly popular in vibration control applications as they provide excellent actuation and sensing capabilities. These properties were discovered more than a hundred years ago by Pierre and Jacque Curie who found that when a strain is applied to a piezoelectric material, a resulting electric charge is produced (this is often referred to as the "direct effect"), and conversely an applied electric field results in a strain (also known as the "converse effect").

Piezoelectricity, which literally means "pressure electricity", is found naturally in many monocrystalline materials, such as quartz, tourmaline, topaz and Rochelle salt. However their effect is generally too weak to be seriously considered in practice. Instead, man-made polycrystalline ceramic materials, such as lead zirconate titanate (PZT), can be processed to exhibit significant piezoelectric properties. PZT ceramics are relatively easy to produce, and are widely as actuators due to their high electro-mechanical coupling factor, which enables them to produce comparatively large forces or displacements from relatively small input voltages and *vice versa*.

The fact that piezoelectric transducers respond to an applied electric field or to an applied strain allows them to be used, respectively, as actuators and sensors and in some cases as both (Fleming, 2004). A general electric representation of a piezoelectric transducer can be modeled as a capacitor (C_p) in series with a strain dependent voltage source (Dosch *et al.*, 1992).

Piezoelectric transducers come in many shapes and forms and can be used in many different applications such as positioning and structural

[1] This research was supported by the Australian Research Council, and the Center for Complex Dynamics Systems and Control.

vibration control. Even though these materials have been successfully used in many engineering applications they suffer from several nonlinearities, such as hysteresis, creep and ageing; the most significant being hysteresis. This nonlinear phenomenon has been well documented (Main and Garcia, 1997) and is of concern when piezoelectric transducers are used as *actuators* and driven by relatively large voltages.

This paper will first define hysteresis in Section 2 and considers different compensation techniques. Section 3 will investigate the implications of using charge to drive piezoelectric actuators on resonant structures. A model will be derived, which can be used to design active controllers as illustrated by the *LQG* approach in Section 4. Experimental results performed on a multivariable cantiliver beam will be presented in Section 5 , after which this paper will be concluded in Section 6.

2. HYSTERESIS AND COMPENSATION

Hysteresis is the major form of nonlinearity present in piezoelectric transducers. The original meaning of the word refers to "lagging behind" or "coming after", however it must not be confused with "phase lag" which is not a nonlinearity and is present in many linear system. The input-output signals coming in and out of a hysteretic system will show sharp reversal peaks at its extremum values, i.e. the derivative of the input and output signals always have the same sign, whereas the tips of a linear system will be more rounded and will display the overall shape of an ellipse. These two behaviors are not mutually exclusive. In fact they often occur together, especially when piezoelectric transducers are bonded or attached to a mechanical structure. Nevertheless a clear distinction must be made between the two.

The level of hysteretic distortion will also vary depending on either the maximum value of the input voltage being applied or the frequency of the input signal or both. The latter case is referred to as "dynamic" or "rate dependent" hysteresis (Mrad and Hu, 2002).

Different approaches have been used to model hysteresis in piezoceramics. The two most notable being the classical Preisach hysteresis model (Mayergoyz, 1991), and the Maxwell resistive capacitor (MRC) model (Goldfarb and Celanovic, 1997). Once a model is obtained its inverse can be derived and used in a feed-forward inverse compensation scheme.

Another method is to use charge or current sources to drive piezoelectric actuators, which have been shown to naturally minimize the effects of hysteresis (Comstock, 1981) as well as increase

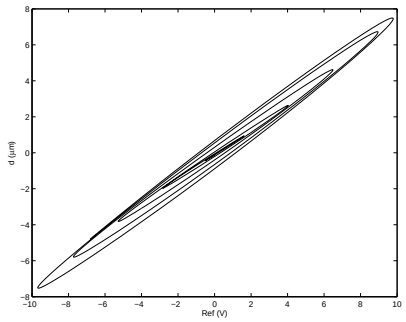

(a)

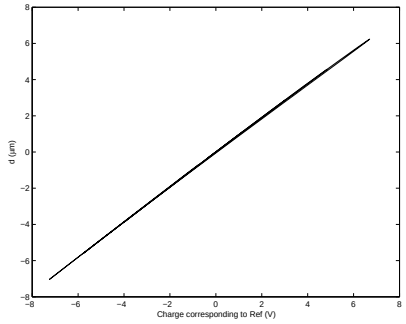

(b)

Fig. 1. Displacement versus a) voltage and b) charge plots measured on a piezoelectric tube

the gain and phase margins of the controlled system (Main and Garcia, 1997). The perceived implementation complexity of such circuits has refrained their wide acceptance. The main problem being that the circuit offsets often result in the load capacitor being charged up. Recently a solution to this problem has been presented by Fleming and Moheimani (Fleming and Moheimani, 2003), in which they use a compliance feedback loop in the current amplifier to estimate and reject all DC offsets. The effectiveness of such an arrangement was demonstrated experimentally by applying a $100Hz$ sinusoidal charge signal followed by a voltage signal to a piezoelectric tube, which is similar to the ones used in AFMs. The amplitude of the charge input was adjusted to obtain the same output displacement magnitude. The input-output results for each case are shown in Figure 1, and clearly demonstrates that electrical charge considerably reduces hysteresis in piezoelectric actuators. A framework for using electrical charge in structural vibration control applications will be explained in the following section.

3. STRUCTURAL VIBRATION CONTROL

Piezoelectric transducers have been extensively used in structural vibration control applications. The reason for this can be attributed to their excellent actuating and sensing capabilities,as well as their non-obtrusive nature.

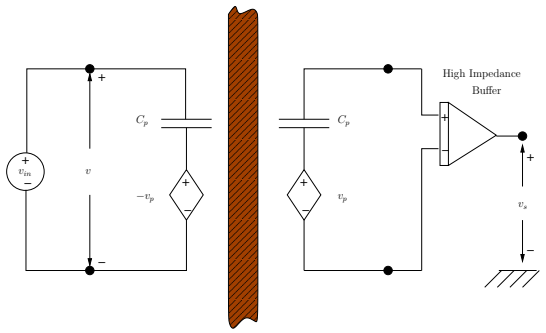

Fig. 2. Voltage driven collocated piezoelectric pair with high impedance buffer

The type of structures, which lend themselves to piezoelectric transducers are generally flexible in nature, such as beams, and plates that are very lightly damped, and are therefore easily susceptible to external disturbances.

The purpose of structural vibration control is to minimize the effect of disturbances acting on a structure in order to extend its operational life span. This can be achieved by effectively increasing the damping of the structure using control feedback.

It will be demonstrated that if current or charge is to be used to drive piezoelectric actuators, the structure of the controllers need to be modified accordingly.

3.1 Voltage Driven Piezoelectric Actuators

The coupled piezoelectric-flexible structure dynamics is well defined for the voltage driven case. It is first covered here in order to lead into the charge driven scenario in the following section.

Piezoelectric actuators and sensors are often collocated in structural vibration control applications. The electrical schematic of this setup for the voltage case is illustrated in Figure 2.

Let G_{vv} be defined as the linear transfer function from input voltage (v_{in}) driving the piezoelectric actuator, to the induced voltage signal (v_p) at the collocated sensor patch. In practice it is physically impossible to directly measure the sensor voltage v_p, therefore the voltage v_s is measured instead using a high impedance buffer (Figure 2) to avoid large measurement errors at low frequencies. G_{vv} is generally obtained experimentally using low input voltages as hysteresis at these levels is negligible

3.2 Charge Driven Piezoelectric Actuators

In order to derive the dynamics of the coupled charge driven piezoelectric actuators and flexible beam, the voltage amplifier in Figure 2 will be replaced by a charge source. The following multi-variable parameters are defined as:

$$V = \begin{bmatrix} v_1 \\ v_2 \\ \vdots \\ v_m \end{bmatrix}; \quad V_p = \begin{bmatrix} v_{p_1} \\ v_{p_2} \\ \vdots \\ v_{p_m} \end{bmatrix}; \quad W = \begin{bmatrix} w_1 \\ w_2 \\ \vdots \\ w_\ell \end{bmatrix};$$

$$\Lambda = \begin{bmatrix} \frac{1}{C_{p_1}} & & & \\ & \frac{1}{C_{p_1}} & & \\ & & \ddots & \\ & & & \frac{1}{C_{p_m}} \end{bmatrix}; \quad Q = \begin{bmatrix} q_1 \\ q_2 \\ \vdots \\ q_m \end{bmatrix}.$$

where V is the voltage applied to the piezoelectric actuators, V_p is the voltage measured from the piezoelectric sensors, W is the disturbance acting on the beam, C_{p_i} is the capacitance associated with each collocated piezoelectric patch and Q represents electrical charge.

Te following assumptions are made:
(i) m piezoelectric actuator/sensor pairs are bonded to the structure;
(ii) Each pair consists of two identical transducers, however, not all transducer pairs are necessarily identical;
(iii) ℓ disturbances are acting on the structure;
(iv) C_{p_i} represents the capacitance of the i^{th} transducer.

Writing the KVL around the left hand loop of Figure 2 for the charge driven case, yields:

$$V = -V_p + \Lambda Q. \tag{1}$$

Furthermore, it can be shown (Vautier, 2004) that the voltage and charge driven closed loop dynamics of a flexible system will be the same as long as:

$$K_q(s) = \Lambda^{-1}(K_v(s) - I). \tag{2}$$

where K_q and K_v correspond to the multi-variable charge and voltage controllers respectively, and the underlying systems are linear.

This means that past research on controller designs and stability analysis for voltage driven piezoelectric actuators can be directly applied to the charge driven case by using (2).

3.3 Coupled Piezoelectric-Beam Model

For the purpose of structural vibration control a good model of the coupled piezoelectric-beam system needs to be obtained. The flexible structure used in the experiments, is a cantilever beam with two collocated piezoelectric pairs attached

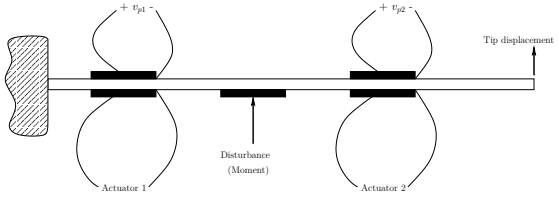

Fig. 3. Beam layout as used in the experiments

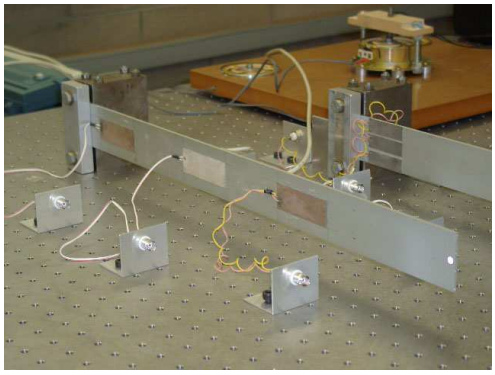

Fig. 4. Picture of the cantilever beam

to it. One pair was located close to the clamped end and the other closer to the free end of the beam. For each collocated pair, one piezoelectric patch was used as an actuator, while the voltage induced in the other patch was used as the sensor. Another piezoelectric actuator was bonded to the beam somewhere between the two actuating patches. This last transducer was driven by a voltage source to apply a disturbance (w) to the beam. A schematic of the beam setup is shown in Figure 3, and a picture of the actual beam is shown in Figure 4.

When driven by voltage this setup can be modelled by the following state space equations:

$$\dot{x}(t) = Ax(t) + B_w w(t) + B_v V(t) \quad (3)$$

$$y_{tip}(t) = C_y x(t) + D_{yw} w(t) + D_{yv} V(t) \quad (4)$$

$$V_p(t) = C_v x(t) + D_{vw} w(t) + D_{vv} V(t) \quad (5)$$

where $x \in \mathbf{R}^{2N}$ represents the state vector of the system; N is the number of modes included in the model, w and $V = \begin{bmatrix} v_1 & v_2 \end{bmatrix}$ represent the disturbance and control input voltages respectively, and y_{tip} and $V_p = \begin{bmatrix} v_{p1} & v_{p2} \end{bmatrix}$ the measured tip displacement and induced voltages.

Substituting (1) into (5) yields:

$$\begin{aligned} V(t) = &-(I + D_{vv})^{-1} C_v x(t) \\ &-(I + D_{vv})^{-1} D_{vw} w(t) \\ &+(I + D_{vv})^{-1} \Lambda Q(t) \end{aligned} \quad (6)$$

Equation (6) can now be used in equations (3)-(5) to obtain the multi-variable state space representation for the plant when the control patches are driven by charge sources. See (Vautier, 2004) for more details.

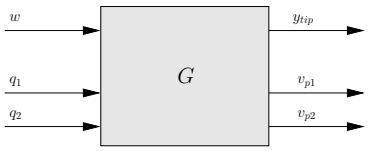

Fig. 5. Augmented MIMO plant

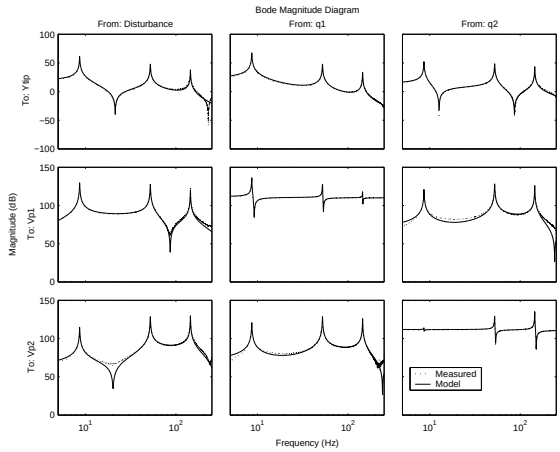

Fig. 6. Identified model with measured data

3.4 Model and System Identification

An optimization based identification technique was used to obtain a structured model of the plant.

A three-input-three-output multi-variable model, of the plant shown in Figure 3 was identified. The representation of the plant in block diagram form is illustrated in Figure 5. The input disturbance w and the output tip displacement y_{tip} are included in the model, as the ratio of these signals (i.e. $G_{yw} = y_{tip}/w$) will be used as a performance indicator. The second and third inputs (q_1 and q_2) in Figure 5 correspond to the charges applied to the first and second actuators, and the second and third outputs are the induced voltages (v_{p1} and v_{p2}) measured at the first and second piezoelectric sensors, respectively.

The plant model was obtained from nine measured frequency responses corresponding to each input-output combination. An optimization problem was framed to obtain the "best fit" state space model by minimizing the normalized least squared error between the simulated and measured frequency data.

The Bode magnitude plots are illustrated in Figure 6, and demonstrate that the identified model closely matches the experimentally measured data.

4. *LQG* CONTROLLER DESIGN

The identified model will facilitate the design of fully multi-variable, two-input-two-output active

charge controllers. The goal of these controllers is to negate the effects of external disturbances acting on the beam by increasing the effective damping of the structure.

An *LQG* controller can be obtained by first designing a state feedback controller K_q and a Kalman state Observer O.

By the Certainty Equivalence Principle (Skogestad and Postlethwaite, 1996) the optimum regulator K_q and observer O can be determined independently. The design of K_q will be considered first, followed by the observer O.

The design objective for the controller is to increase the damping of the structure by regulating the tip displacement y_{tip} of the cantilever beam. In a linear quadratic sense J needs to be minimized:

$$J = \int_0^\infty \left[y_{tip}(t)^2 + \ Q'(t) K_u Q(t) \right] \ dt \qquad (7)$$

where K_u is a 2×2 weighting matrix on the applied charge control signals Q.

From 7, one can easily derive the standard *LQR* deterministic cost function for the system:

$$J = \int_0^\infty \left\{ x'(t) P x(t) + \ Q'(t) R Q(t) \right\} \ dt \qquad (8)$$

where $P = \tilde{C}_y' \tilde{C}_y$, $R = K_u$

P and R represent the performance and controller input weightings respectively, and $\tilde{C}_y$ corresponds to the *charge* driven output tip displacement matrix.

To effectively reduce the tip displacement of the beam an extra scalar weighting (α) was added to P such that $P = \alpha \tilde{C}_y' \tilde{C}_y$.

The optimum state feedback controller K_q that minimizes J is obtained by solving the corresponding Algebraic Riccati Equation.

Since we are only measuring the voltage sensors V_p a Kalman observer O was designed to estimate the states of the plant, such that it minimized:

$$J_o = E\left\{ \left[x(t) - \tilde{x}(t) \right]' \left[x(t) - \tilde{x}(t) \right] \right\} \qquad (9)$$

where x and $\tilde{x}$ are the exact and estimated states of the plant respectively and E is the expectation operator.

The following assumptions were made. The disturbance (w) and the measurement noise (v) are uncorrelated zero-mean Gaussian stochastic processes with constant power spectral density matrices $\mathcal{P}_n$ and $\mathcal{R}_n$ respectively. Therefore the covariances of w and v are:

$$E\left\{ w(t) w'(t) \right\} = \mathcal{P}_n \qquad (10)$$

$$E\left\{ v(t) v'(t) \right\} = \mathcal{R}_n \qquad (11)$$

and $E\left\{ w(t) v'(t) \right\} = 0 \ , \ E\left\{ v(t) w'(t) \right\} = 0$

A Kalman observer O that minimizes (9) can then be found by solving an algebraic Riccati equation, based on $\mathcal{P}_n$ and $\mathcal{R}_n$.

The observer O and state feedback controller K_q are then coupled to form the augmented controller $C(s)$. The parameters α, K_u, $\mathcal{P}_n$ and $\mathcal{R}_n$ are simply used as design parameters. Several simulation with different values for the parameters are performed and the combination that offers the best compromise between stability and damping is chosen.

The corresponding Bode plot of the controller is shown in Figure 7.

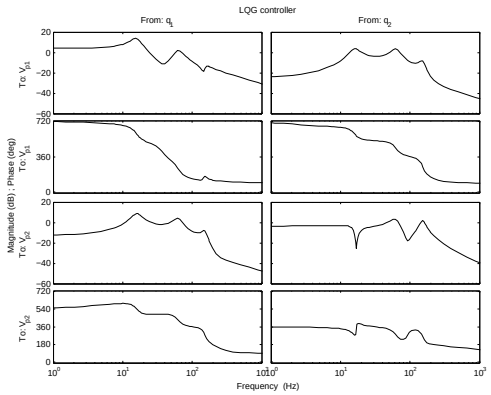

Fig. 7. *LQG* controller

5. EXPERIMENTAL SETUP AND RESULTS

The experiments were performed on a cantilever Euler Beam as shown in Figure 4. As previously mentioned, the disturbance voltage was applied to a secondary patch located at the center of the beam and the two collocated actuator-sensor pairs were used for feedback control purposes only. A Polytec laser scanning vibrometer (PSV-300) with a set sampling rate of 1.024 kHz, was used to measure the velocity at the tip of the beam. The experimental open and closed loop frequency responses were obtained by applying a sinusoidal voltage signal of varying frequency to the "disturbance" piezoelectric patch and measuring the corresponding output tip displacement of the beam (y_{tip}), with and without the controller being switched on. The controller was downloaded from Simulink onto a dSPACE DS-1103 DSP board. Low-pass, anti-aliasing, and reconstruction filters were added to the system. The measured voltage for each piezoelectric sensor was passed through a high-impedance buffer, which ensures the sensor signals remain accurate at low frequencies.

The open and closed loop Bode magnitude plots for the experimental and simulation results are

shown in Figure 8. The displacement step response results can be found in Figure 9. A summary of the results is shown in Table 1.

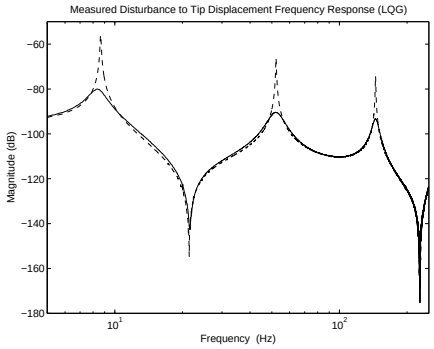

(a) Measured Data

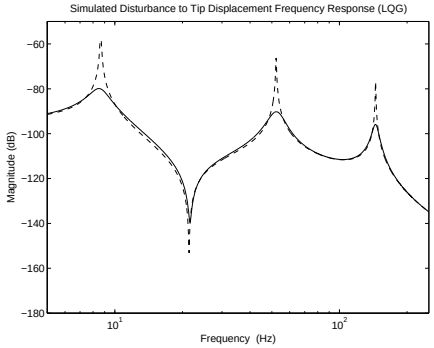

(b) Simulation Results

Fig. 8. Open and closed loop frequency response for input disturbance w to output tip displacement y_{tip} using a LQG controller

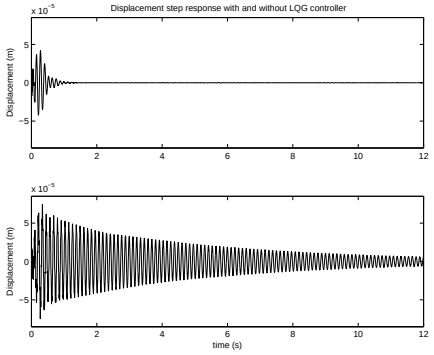

Fig. 9. Displacement step response at the tip of the beam with and without the LQG controller

Table 1. Peak reduction and damping ratios using the LQG controller

LQG results	Modes		
	1^{st}	2^{nd}	3^{rd}
Peak reduction (dB)	24	23.8	18.9
Open loop damp. ratio (10^{-3})	3.28	3.29	2.40
Closed loop damp. ratio (10^{-3})	94.7	98.9	30.5

The results shown are satisfactory, and demonstrate that charge driven piezoelectric actuators can be successfully implemented using robust control design strategies.

6. CONCLUSIONS

Electrical charge is known to naturally reduce the negative effects of hysteresis when used to drive piezoelectric actuators. The implications for using this method in structural vibration control applications were investigated. The analysis revealed that the dynamics of a piezoelectric-beam model were different when charge, rather than voltage, was used to drive piezoceramic actuators. A multivariable LQG charge controller was designed and experimentally validated on a flexible cantilever beam. The results clearly demonstrate that charge driven piezoelectric actuators can be successfully used to reject unwanted vibrations from flexible structures.

REFERENCES

Comstock, R. H. (1981). Charge control of piezoelectric actuators to reduce hysteresis effects. *United States Patent.*

Dosch, J. J., D. J. Inman and E. Garcia (1992). A self-sensing piezoelectric actuator for collocated control. *Journal of Intelligent Material Systems and Structures* **3**, 166–185.

Fleming, A. J. (2004). Synthesis and implementation of sensor-less shunt controllers for piezoelectric and electromagnetic vibration control. PhD thesis. School of Electrical Engineering and Computer Science, The University of Newcastle, Australia.

Fleming, A. J. and S. O. R. Moheimani (2003). Precision current and charge amplifiers for driving highly capacitive piezoelectric loads. *IEE Electronics Letters* **39**(3), 282–284.

Goldfarb, M. and N. Celanovic (1997). A lumped paramater electromechanical model for describing the nonlinear behavior of piezoelectric actuators. *Journal of Dynamics Systems, Measurement, and Control* **119**, 478–485.

Main, J. A. and E. Garcia (1997). Piezoelectric stack actuators and control system design: Strategies and pitfalls. *Journal of Guidance, Control and Dynamics* **20**(3), 479–485.

Mayergoyz, I. (1991). *Mathematical Models of Hysteresis*. Springer-Verlag.

Mrad, R. B. and H. Hu (2002). A model for voltage to displacement dynamics in piezoceramic actuators subject to dynamic voltage excitations. *IEEE/ASME Transactions of Mechatronics* **7**(4), 479–489.

Skogestad, S. and I. Postlethwaite (1996). *Multivariable Feedback Control*. John Wiley and Sons.

Vautier, B. J. G (2004). Charge-driven piezoelectric actuators in structural vibration control applications. Master's thesis. School of Electrical Engineering and Computer Science, The University of Newcastle, Australia.